



Published in final edited form as:

*Virology*. 2008 February 20; 371(2): 336–349. doi:10.1016/j.virol.2007.09.030.

## Intracellular trafficking pathway of BK virus in human renal proximal tubular epithelial cells

Takahito Moriyama and Andrey Sorokin \*

*Division of Nephrology and Kidney Disease Center, Department of Medicine, Medical College of Wisconsin, Milwaukee, WI 53226, USA*

### Abstract

Intracellular trafficking of BK Virus (BKV) in human renal proximal tubular epithelial cells (HRPTEC) is critical for BKV nephritis. However, the major trafficking components utilized by BKV remain unknown. Co-incubation of HRPTEC with BKV and microtubule disrupting agents prevented BKV infection as detected by immunofluorescence and western blot analysis with antibodies which recognize BKV large T antigen. However, inhibition of a dynein, cellular motor protein, did not interfere with BKV infection in HRPTEC. A colocalization study of BKV with the markers of the endoplasmic reticulum (ER) and the Golgi apparatus (GA), indicated that BKV reached the ER from 6 to 10 hours, while bypassing the GA or passing through the GA too transiently to be detected. This study contributes to the understanding of mechanisms of intracellular trafficking used by BKV in the infection of HRPTEC.

### Keywords

BK Virus; polyoma virus; human renal proximal tubular epithelial cells; microtubules; microtubules dynamicity, dynein; endoplasmic reticulum; golgi apparatus

## INTRODUCTION

To elucidate the details of pathogenesis of viral disease, progress of viral infection, and efficient therapeutic strategy, investigation of viral life cycle is necessary. In most types of viruses, a specific receptor is used to attach to the cell surface and enter into the cytoplasm via a clathrin-mediated endocytosis pathway (Damm and Pelkmans, 2006; Marsh and Helenius, 2006; Pelkmans and Helenius, 2003). After penetration through clathrin coated pits, clathrin-coated vesicles move along the microtubules, are transported to early endosomes by membrane fusion and then delivered to the late endosomes and lysosomes. Transportation of some viruses along the microtubules is dependent on the activity of the microtubule motor protein dynein. After viruses reach the nuclear membrane, the viral genome is released into the nucleus, DNA replication occurs, and daughter viruses are released when the cells are lysed. With regard to polyoma viridae, JC Virus has been reported to enter into cells via clathrin coated pits (Pho et al., 2000), but simian virus 40 (SV40), mouse polyoma virus (mPy), and BK Virus (BKV)

\*Corresponding author Mailing address: Division of Nephrology and Kidney Disease Center, Department of Medicine, Medical College of Wisconsin, 8701 Watertown Plank Road, Milwaukee, WI 53226, USA Phone: 414-456-4438 Fax: 414-456-6515 E-mail: E-mail: sorokin@mcw.edu.

**Publisher's Disclaimer:** This is a PDF file of an unedited manuscript that has been accepted for publication. As a service to our customers we are providing this early version of the manuscript. The manuscript will undergo copyediting, typesetting, and review of the resulting proof before it is published in its final citable form. Please note that during the production process errors may be discovered which could affect the content, and all legal disclaimers that apply to the journal pertain.

have been reported to enter into cells via caveolae mediated endocytosis pathway (Chen and Norokin, 1999; Eash et al., 2004; Gilbert and Benjamin, 2000, 2004; Moriyama et al., 2007; Nichols, 2003; Pelkmans et al., 2001; Pelkmans and Helenius, 2002, 2003; Pelkmans, 2005; Pietiäinen et al., 2005; Pfeffer, 2001; Richterová et al., 2002). A number of studies have focused on the intracellular trafficking pathway of SV40, mPy, and BKV after caveolae endocytosis (Ashok and Atwood, 2003; Bernacchi et al., 2004; Eash and Atwood 2005; Gilbert and Benjamin, 2004; Gilbert et al., 2003; Norkin et al., 2002; Norkin and Kuksin, 2005; Tagawa et al., 2005), but little is known about the intracellular trafficking pathway of BKV after caveolar mediated endocytosis into HRPTEC.

For SV40, virus particles were trapped in caveolae, were coated with caveolin-1 containing membrane, surrounded by monomeric actin and pinched off (Chen and Norkin, 1999; Pelkmans and Helenius, 2003; Pfeffer, 2001). Subsequently, caveolin-1 coated SV40 particles fused with caveosomes which were positive for caveolin-1 and did not contain any markers of lysosomes and endosomes, and then moved along microtubules (Bernacchi et al., 2004; Norkin et al., 2002). Transportation of SV40 required intact functional microtubules (Zhou et al., 1995), but it did not rely on the motor protein dynein (Ashok and Atwood, 2003). After several hours, SV40 had reached to the endoplasmic reticulum (ER), but bypassed the Golgi apparatus (GA) (Bernacchi et al., 2004; Damm and Pelkmans, 2006; Norkin and Kuksin, 2005; Pelkmans et al., 2001, 2002; Pelkmans and Helenius, 2002; Pelkmans, 2005; Pietiäinen et al., 2005; Radtke et al., 2006; Richards et al., 2002; Richterová et al., 2002; Sanjuan et al., 2003; Tagawa et al., 2005).

Endocytosis of mPy was reported to depend on its cell type. mPy entered into murine fibroblasts and primary baby mouse kidney epithelial cells through a caveolae and clathrin-independent pathway (Gilbert and Benjamin, 2000; Gilbert et al., 2003) while entering normal murine mammary gland epithelial cells via caveolae-dependent pathway (Sanjuan et al., 2003). Whether or not endocytosis depended on caveolae, mPy particles were reported to be transported along microfilaments and microtubules, and delivered to the ER, but not to the GA (Gilbert et al., 2003; Gilbert and Benjamin, 2004; Hamm-Alvarez et al., 1994, 1996; Sanjuan et al., 2003).

With regard to BKV, we previously reported that BKV entered into HRPTEC through caveolae (Moriyama et al., 2007). After internalization through caveolae, BKV particles were fused with each other and became clusters of vesicles called caveosome (Drachenberg et al., 2003). The BKV intracellular trafficking pathway in Vero cells was reported to include transportation along microtubules, but BKV movement was not dependent upon microtubules dynamics (Dugan et al., 2006; Eash and Atwood, 2005). BKV was also reported to be transported to the ER before reaching the nucleus, since brefeldin A, an inhibitor of protein trafficking from the ER to the GA, interfered with BKV infection in HRPTEC, and the ER membrane contained receptors for BKV (Low et al., 2006).

However, it is yet to be determined whether intracellular trafficking pathway of BKV particles in their natural target cells, HRPTEC, requires intact and dynamic microtubules. Additionally, has not been determined whether dynein, a microtubule motor protein which mediates transportation of several types of viruses, is required for the transportation of BKV. Although BKV is transported to the ER in HRPTEC, it is still unclear whether BKV is transported to the GA. In this study, we examined the intracellular trafficking pathway of BKV using several pharmacological agents. Nocodazole (Noc) and colcemid (Col) were used as microtubule depleting agents. Paclitaxel (Pac) was used as a microtubule stabilizing agent (it also depleted the dynamics of microtubules), and erythro-9-(2-hydroxy-3-nonyl) adenine hydrochloride (EHNA) as a dynein inhibitor. We also examined colocalization of cesium chloride (CsCl)-

purified and labeled BKV with the ER and/or the GA. Our data provide a detailed analysis of the intracellular trafficking pathway of BKV in HRPTEC.

## RESULTS

### The role of microtubules in BKV infection

BKV particles were shown to move along the microtubules in monkey derived Vero cells (Dugan et al., 2006; Eash and Atwood, 2005). In order to investigate the precise mechanism of BKV uptake pathway in humans, we used microtubule disrupting agents Noc and Col in HRPTEC, which are main target of BKV infection in actual BKV clinical situation.

In control HRPTEC cells (untreated or incubated only with microtubule disrupting agents) immunofluorescence (IF) analysis did not reveal any T-Ag positive cell. When HRPTEC were incubated with BKV alone, the percentage of infected cells were  $36.68 \pm 1.47\%$ . But when HRPTEC were co-incubated with BKV and several doses of Noc (6.25, 12.5, 25, and 50  $\mu\text{M}$ ), the percentage of infected cells was significantly decreased in comparison to HRPTEC incubated with BKV alone ( $P < 0.001$ ), and there was a significant decreasing trend with increasing dose of Noc ( $P < 0.001$ ) (Figure 1A). In western blot (WB) analysis, there was no T-Ag expression in control groups (untreated HRPTEC and HRPTEC incubated with Noc alone) as expected. In HRPTEC, co-incubated with BKV, increasing doses of Noc decreased the relative T-Ag expression when compared to HRPTEC incubated with BKV only ( $P < 0.001$ ) (Figure 1B).

Figure 2A showed that the percentage of BKV infected cells was significantly lower when HRPTEC were co-incubated with BKV plus several doses of Col ( $P < 0.001$ ) when compared to HRPTEC incubated with BKV alone. There was also a significant decreasing trend with increasing dose of Col ( $P < 0.001$ ). Figure 2B shows the significant differences in relative T-Ag expression when HRPTEC were incubated with BKV alone compared to HRPTEC co-incubated with BKV and several doses of Col ( $P < 0.001$ ). This significant trend of decreasing T-Ag expression also continued when HRPTEC were incubated with BKV and several doses of Col ( $P < 0.001$ ).

These results indicate that BKV moves along with microtubules in HRPTEC which is similar to transportation of BKV in Vero cells.

### Effect of dynamics of microtubules on BKV infection

It has been reported that transportation of BKV along microtubules did not require dynamics of microtubules in Vero cells (Dugan et al., 2006; Eash and Atwood, 2005). However, since the role of microtubule dynamics for BKV transportation in HRPTEC has not been elucidated, we investigated its potential role in HRPTEC using treatment with Pac, which disrupted microtubules dynamics.

The percentage of BKV infected cells detected by IF analysis, was significantly lower when HRPTEC were co-incubated with BKV and several doses of Pac ( $P < 0.001$ ), in comparison to HRPTEC incubated with BKV alone (Figure 3A), and there was also a significant decreasing trend with increasing dose of Pac ( $P < 0.001$ ). In WB analysis, relative T-Ag expression was significantly lower in HRPTEC with BKV and higher doses of Pac ( $P < 0.001$ : 5, 10, and 20  $\mu\text{M}$ ), in comparison to HRPTEC incubated with BKV alone, and there was a significant decreasing trend with dose ( $P < 0.001$ ) (Figure 3B).

These data suggest that dynamics of microtubules plays an important role for transportation of BKV in HRPTEC, which is different from what was demonstrated in Vero cells.

### Dynein was not required for the BKV transportation

Dynein is the motor protein on the microtubules and it plays an important role for the transportation of the vesicles, granules, and molecules along the microtubules in the cytoplasm. Several viruses also have been reported to be transported by this motor protein (Greber and Way, 2006; Leopold and Pfister, 2006; Radtke et al., 2006). To evaluate the role of dynein, we have used EHNA. EHNA has been known as an inhibitor of adenosine triphosphate (ATP)ase activity of the dynein complex which correlates with dynein motility (Bouchard et al., 1981; Cheung et al., 2004; Dhani et al., 2003).

Figure 4A showed that the percentage of BKV infected cells was not significantly different between HRPTEC incubated with BKV alone and HRPTEC co-incubated with BKV and several doses of EHNA. Figure 4B also showed no differences in relative T-Ag expression between HRPTEC incubated with BKV alone and those co-incubated with BKV and EHNA. Inhibition of the dynein motor function results in disruption of GA which is accompanied by a dramatic distribution of GA markers to dot-like structures (Ashok and Atwood, 2003; Arsaki et al., 2007; Burkhardt et al., 1997; Cheung et al., 2004; Presley et al., 1997). Figure 4C demonstrates that EHNA was efficient in inhibition of dynein function in HRPTEC in our experiments as revealed by re-localization of GA marker. GA was seen as located perinuclear cisterna in untreated HRPTEC, whereas treatment with EHNA caused dispersal of the GA (Figure 4C). Therefore, as expected, EHNA was efficient in inhibiting the motor function of dynein in HRPTEC. These results indicate that dynein function is dispensible for BKV infection of HRPTEC.

### Colocalization of labeled and purified BKV with ER or GA

Figure 5A shows the colocalization of Alexa Fluor™ 488 labeled and CsCl purified BKV (green) with the ER (red). HRPTEC were incubated with BKV at MOI 5 FFU/cell from 2 to 16 hours. At 2 hours, a few BKV particles were located on the cell surface. No colocalization of BKV particles with ER was observed at this time. At 4 hours, some BKV particles were located on the cell surface and the others in the cytoplasm, and viral particles started to colocalize with the ER. At 6 and 8 hours, a majority of BKV particles were located in the cytoplasm, and several viral particles were colocalized with the ER. After 10 hours incubation, almost all BKV particles were located in the cytoplasm, and some of them were colocalized with the ER, but others were located in the perinuclear cisterna. Figure 5B shows the colocalization of labeled BKV with the GA. Throughout the incubation period, labeled BKV were not seen adjacent to the GA, though a lot of BKV particles were located in the perinuclear cisterna and a few particles were located in the nucleus after 6 hours. Figure 5C showed the colocalization rate of BKV and the ER or the GA. Colocalization rate of BKV and the ER was increased gradually from 2 to 6 hours, peaked at 6 hours incubation ( $13.29 \pm 1.68\%$ ), and tapered off after 8 hours incubation. Colocalization rate of BKV with the ER at 6,8,10, and 12 hours were significantly higher than at 2 hours ( $p < 0.001$ ). Colocalization rate of BKV with the GA also remained low all through the incubation period, and significantly lower than colocalization rate of BKV and the ER at 6, 8, 10, 12, and 14 hours ( $p < 0.0001$ : 6 and 8 hours,  $p < 0.001$ : 10 and 12 hours, and  $p < 0.01$ : 14 hours). Colocalization rate of BKV particles with caveolin-1 (major structural component of caveolae) (Moriyama et al., 2007) is also shown to illustrate the fact that prior to arrival at the ER, BKV particles are associated with caveolae.

These results indicate that BKV reaches the ER mostly at 6 to 8 hours after infection, but bypasses the GA or passes through the GA at times points other than those which we studied. The intracellular trafficking pathway of BKV is similar to those used by other polyoma viruses, SV40 and mPy.

## DISCUSSION

A few previous studies addressed the uptake pathways utilized by BKV in a number of mammalian cells. Previous reports indicated that gangliosides GD1b and GD1b played a pivotal role as a receptor of BKV in human prostate carcinoma cells and BKV passed through the ER before reaching the nucleus in HRPTEC (Low et al., 2006). Atwood *et al.* reported that N-linked glycoprotein with  $\alpha$  (2, 3)-linked sialic acid served as a receptor for BKV (Dugan et al., 2005). BKV entry involved a caveolae-mediated pathway (Eash et al., 2004), and required microfilament dynamics and intact microtubules, but not actin filaments and dynamic state of the microtubules filaments in the early steps of viral infection in monkey derived Vero cells (Eash and Atwood, 2005). We have previously reported that BKV entered HRPTEC through caveolae, but not through clathrin coated pits, and BKV particles were routinely trapped in caveolae at 4 hours after infection (Moriyama et al., 2007). However, the details and kinetics of the intracellular trafficking pathway employed by BKV, following endocytosis through caveolae, have not been fully understood, particularly in cells naturally targeted by BKV (HRPTEC). In this study, we showed the time course of BKV intracellular trafficking from microtubules to the ER (bypassing the GA) and evaluated the role of microtubule dynamics and the motor protein dynein in BKV infection of HRPTEC.

Initially, we focused on the role of intact microtubules and their dynamics in BKV transportation in the cytoplasm of HRPTEC. Microtubules are cytoskeletal filaments consisting of  $\alpha$ - and  $\beta$ -tubulin dimers, and their function is to determine intracellular structure for the maintenance of cell shape, cell motility, as well as intracellular transport of molecules, vesicles and granules between organelles. Microtubule dynamics consist of shrinking and growing of tubulin dimers at microtubule ends, and this is essential for the separation and movements of chromosomes on the mitotic spindle. Interestingly, previous reports suggested that mPy and SV40 were transported along microtubules after caveolae endocytosis (Bernacchi et al., 2004; Gilbert and Benjamin, 2004; Gilbert et al., 2003; Norkin et al., 2002; Tagawa et al., 2005). BKV moved along the microtubules in Vero cells (Eash et al., 2004), but the dynamics of microtubules was not required for the transportation of BKV (as well as mPy) in contrast to SV40 (Zhou et al. 1995). We used Noc and Col as microtubule disrupting agents, and Pac as microtubule dynamics disrupting agents. Noc disrupts microtubules by binding to  $\beta$ -tubulin and preventing formation of one of the two interchain disulfide linkages. Col is related to colchicine but it is less toxic. Col depolymerises microtubules and limits microtubule formation. Pac has the opposite effect of Noc and Col and binds to the N-terminal region of  $\beta$ -tubulin, promoting the formation of highly stable microtubules that resist depolymerization, and suppresses the dynamics of microtubules. Colchicine and Pac are actually used in the treatment of cancer. Our results showed all three agents interfered with BKV infection in HRPTEC, indicating that transportation of BKV required not only intact microtubules, but also their dynamics. Our data suggesting the BKV requirement for intact microtubules support previously reported data about mPy, SV40, and BKV intracellular transportation, but with regard to the dynamics of microtubules, our results were different from those reported for mPy and BKV in Vero cells (Bernacchi et al., 2004; Eash et al, 2005; Gilbert and Benjamin, 2004; Gilbert et al., 2003; Norkin et al., 2002; Tagawa et al., 2005). Eash *S et al.* reported that suppression of the microtubules dynamicity did not interfere with BKV infection in Vero cells (Eash et al., 2005). These discrepancies may be explained by the fact, that different cells were used in these studies. In a similar manner to our results, transportation of SV40 in CV-1 cells was reported to be inhibited by Pac, indicating that the dynamics of microtubules was required for transportation of SV40 (Zhou et al., 1995). Microtubule-dependent vesicle transport was also reported to be inhibited by Pac (Hamm-Alvarez et al, 1993, 1994, 1996; Sonee et al., 1998). Observation that microtubule dynamics was associated with transportation of molecules and viral particles supports our conclusions.

The other factors, which play an important role in the intracellular transportation of vesicles, granules, and molecules, are motor proteins dynein and kinesin, which move cargo along the microtubules. In particular, dynein is a minus-end microtubule motor protein, binds to the microtubule organizing centre (MTOC) near the nucleus, and is known to transport a wide variety of viruses, such as Adenovirus, African swine fever virus, Canin Parvovirus, Foamy virus, Herpes simplex virus, Influenza virus X-31, Lyssavirus, Human immune deficiency virus type1, Rabies virus, and Vaccinia virus, even though these viruses have their own receptor and endocytic pathway (Greber and Way, 2006; Leopold and Pfister, 2006; Radtke et al., 2006). These reports allowed us to hypothesize that BKV transportation along microtubules was dependent upon dynein action. Nevertheless, our results indicated that there was no relationship between the transportation of BKV and dynein activity. It has been reported that other polyoma viruses (JC virus and SV40) also did not require dynein for intracellular transportation (Ashok and Atwood, 2003). Though a lot of viruses are transported by dynein, polyoma viridae appear to progress along microtubules independently of dynein.

Next, we examined the subsequent trafficking pathway of BKV after transportation along the microtubules. A previous report indicated that BKV reached the ER in HRPTEC (Low et al., 2006), but whether BKV passed through the GA, and the time course of intracellular trafficking pathway was not studied. Our colocalization study of purified and labeled BKV with the markers of ER and GA showed that BKV passed through the ER mostly from 6 to 8 hours after infection, but bypassed the GA or passed the GA too rapidly to be detected. These results are similar to those obtained for other polyoma virus, mPy and SV40 (Bernacchi et al., 2004; Gilbert et al., 2003; Norkin et al., 2002; Tagawa et al., 2005), but the course of BKV infection in HRPTEC seemed to be relatively slow. SV40 has been reported to be colocalized with Caveolin-1 most frequently at 0.5 hour and with perinuclear region at 4 hours after infection in CV-1 cells (Pelkmans et al., 2001). mPy has been reported to be colocalized with cav-1 at 0.5 hour, actin at 0.5 to 1 hour, microtubules at 2 to 4 hours, and ER at 4 hours after infection in GD1a-supplemented rat glioma cells (Gilbert and Benjamin, 2004). As for BKV, T-Ag and VP1 protein expression started between 12 to 24 hours after infection and expressed strongly at 36 hours after infection. Viral DNA replication began from 48 hours after infection by Southern blotting analysis (Low et al., 2004). In this study it was also reported that the titer of BKV started to increase at 2 days after BKV infection in HRPTEC. Thus, at least 24-48 hours were necessary for expression of viral proteins and DNA in HRPTEC. These data are in support of our conclusions about the time course of BKV intracellular transport and localization.

Our previous data dealing with colocalization of BKV with caveolin-1 (Moriyama et al., 2007) taken together with the results of our current study allow us to conceive the whole viral life cycle in HRPTEC. In summary, after attachment to the cell surface of HRPTEC, BKV particles move along cell surface, and are trapped in caveolae at 4 hours after infection. After endocytosis via caveolae, they are transported along the microtubules if the dynamics of microtubules is intact. This process seems to be independent of motor protein dynein activity, and BKV reaches the ER at 6 to 8 hours after infection, bypassing the GA or passing through the GA rapidly. BKV particles then presumably enter into the nucleus, viral replication occurs, and daughter viruses are delivered to other cells. This process takes at least 24 to 48 hours and is very similar to SV40 infection in the polyoma viridae.

This is the first report to demonstrate the unique time course of BKV infection and provide evidence of the mechanism of BKV intracellular trafficking in HRPTEC, the main natural target of BKV. Viral life cycles are quite different in each cell type, therefore it is important to employ HRPTEC to elucidate precise mechanisms and kinetics of BKV infection.

## MATERIALS AND METHODS

### Human renal proximal tubular epithelial cells (HRPTEC) culture

HRPTEC, purchased from Cambrex Bio Science Inc. (Walkersville, MD), were cultured as recommended by manufacturer. Briefly HRPTEC were plated for culture in renal epithelial cell basal medium (REBM™) (Cambrex Bio Science Inc.) containing 10 % fetal Bovine serum (FBS), renal epithelial growth media (REGM™) SingleQuots (h epidermal growth factor (hEGF), insulin, hydrocortisone, gentamicin / amphotericin-B (GA)-1000, epinephrine, triiodothyronine, transferring) (Cambrex Bio Science Inc.) and 100 units/ml penicillin-G (Invitrogen, Carlsbad, CA) in a humidified 5% CO<sub>2</sub> incubator at 37 °C. Passage 6 HRPTEC was used in all experiments.

### Viruses (propagation, titer, purification, and labeling)

BKV was purchased from ATCC (Manassas, VA) and was propagated as previously described (Moriyama et al., 2007). Briefly, HRPTEC were infected with BKV for four weeks with medium changed or collected every week. After four weeks, the cells were harvested by scraping. All collected medium and harvested cells were centrifuged at 10,000 rpm for 15 minutes. Pellets were re-suspended in 1/10 of the supernatant, then frozen at -80 °C and thawed at 37 °C three times. To release virus from the nucleus and cytoplasm, the cells were sonicated. Then deoxycholate (Sigma-Aldrich, St. Louis, MO) was added at a final concentration of 0.25 % and incubated at 37 °C for 30 minutes. The lysate and medium mixtures were centrifuged at 10,000 rpm for 30 minutes. Supernatant was saved for experimental use.

Viral titers were calculated as fluorescence forming units (FFU) per ml using fluorescent focus assay (FFA) as previously described (Moriyama et al., 2007). Briefly, 70 % confluent HRPTEC in a 24-well plate were incubated with 10-fold serial dilutions of BKV for 72 hours at 37 °C. Fresh medium was then added and cells were incubated for another 48 hours. Cells were fixed and analyzed by an immunofluorescence method. Infected cells were counted in five random areas of each cover slip, and means ± SE were calculated from three different cover slips of same BKV amount.

Viral purification was achieved as previously described (Moriyama et al., 2007). Virus-containing supernatant was gently layered at the top of 20 % sucrose and centrifuged at 100,000 × g, 4 °C, for 2 hours in 70 Ti Rotor (Beckman, CA). Pellets were dissolved with buffer A (1 M Tris [pH 8], 5M NaCl, 0.1 M CaCl<sub>2</sub>) and sonicated for 30 seconds three times. The sonicated viral sample was overlaid on CsCl density gradient (1.40 and 1.20 g/ml) and ultracentrifuged at 120,000 × g, overnight. The viral fraction was extracted, diluted with buffer A, and ultracentrifuged on CsCl gradient again. The viral fraction was extracted and dialyzed against buffer A at 4 °C overnight. The purified virus was labeled with Alexa Fluor™ 488 Microscale Protein Labeling Kit (Molecular Probes, Eugene, OR) according to the manufacturer's instructions. Briefly, 100 µl of purified viral solution was transferred to a reaction tube and 10 µl of 1M sodium bicarbonate was added. Then 33 nM Alexa Fluor tetrafluorophenyl ester was added to the reaction tube for 15 minutes. After incubation, 50 µl of the conjugate reaction mixture was layered on the resin bed in the microcentrifuge tube and centrifuged at 16,000 × g for 1 minute. The efficiency of BKV infection in HRPTEC was not significantly affected by viral purification and labeling, though these procedures led to decrease of viral titers from 4.8×10<sup>7</sup> FFU/ml to 1.0×10<sup>7</sup> FFU/ml.

### Antibodies and agents

To detect T-Ag, anti-SV40 T antigen (Ab-2) mouse monoclonal antibody (PAb 418) was purchased from Calbiochem (San Diego, CA). These antibodies cross-react with BKV T antigen. Protein disulfide isomerase (PDI) as ER marker, Mannosidase II as Golgi marker, and

GAPDH as loading control were purchased from Abcam (Cambridge, MA). For immunofluorescence (IF) and western blots (WB) analysis by Odyssey® (LICOR, Inc., Lincoln, NE), Alexa flour™ 488 goat anti-mouse IgG (H+L), Alexa flour™ 680 goat anti-mouse IgG (H+L), Alexa flour™ 680 goat anti-rabbit IgG (H+L), 4',6-diamidino-2-phenylindole, dilactate (DAPI, dilactate) (Molecular Probes, Eugene, OR), and IRDye™ 800 conjugated affinity purified anti-rabbit IgG (H&L) (Rockland Immunochemicals Inc., Gilbertsville, PA) were purchased. Pac, Noc, EHNA (Sigma-Aldrich) and Col (Calbiochem) were also purchased.

### Infection and treatment

In experiments using pharmacological agents, passage 6 HRPTEC were pre-incubated with each agent at 37 °C for 1 hour. BKV was then added and co-incubated another 72 hours at 37 °C. After 72 hours co-incubation, the cells were washed and incubated for another 48 hours with medium containing each agent. HRPTEC not incubated with BKV and any pharmacological agents were used as negative control. The concentration of each agent that did not affect cell viability was determined by cytotoxic assay (CytoTox 96® Non-Radioactive Cytotoxicity Assay, Promega, Madison, WI) according to the manufacture's protocol and were used for all experiments.

### Western Blot analysis (WB analysis)

After incubation with BKV and/or inhibitors, cell monolayers were washed three times with phosphate buffered saline (PBS). Cells were scraped and harvested, and these samples were separated by sodium dodecyl sulfate-polyacryl-amide gel electrophoresis (SDS-PAGE) using 10 % Tris-HCl gel (BIO-RAD Laboratories, Hercules, CA). Gel-separated protein bands were blotted onto polyvinylidene difluoride (PVDF) membranes (Millipore Corporation, Bedford, MA). The membranes were blocked in Odyssey® blocking buffer (LI-COR, Inc.) at room temperature for 1 hour. After blocking, the membranes were incubated with primary antibody (PAb 416 and GAPDH) at 4 °C overnight with constant rotation. The membranes were then washed four times with Tris-buffered saline containing 0.1 % Tween-20 (TTBS) at room temperature for 5 minutes with agitation, and incubated with secondary antibody (Alexa flour 680™ and IRDye™ 800). The membranes were washed four times with TTBS at room temperature for 5 minutes with agitation. Bands were visualized by Odyssey® infrared imaging system. Integrated intensity of each signal was measured by Odyssey®, and relative intensity of T-Ag revised by GAPDH was expressed as graph bars.

### Indirect immunofluorescence analysis (IF analysis)

HRPTEC seeded on cover slips were fixed in 100 % methanol at – 20 °C for 20 minutes after 3 times washes with PBS. After incubation in TTBS containing 3 % bovine serum albumin (BSA) for 30 minutes, cells were incubated with primary antibody (1 µg/ml PAb 416, 1:100 dilution of PDI, or 1:200 dilution of Mannosidase II) diluted with TTBS containing 1 % BSA for 1 hour, and washed three times with TTBS for 5 minutes each. Cells were then incubated with secondary antibody (1:200 dilution of Alexa flour™ 488 or 680) for 40 minutes, and washed three times with TTBS for 5 minutes each. To stain nuclei, cells were incubated with DAPI (300 nM) for 5 minutes and washed three times with PBS.

To determine the percentage of infected cells, a fluorescent microscope (Nikon Eclipse E600) was used to observe cells, and SPOT® version 4.0.9 (Diagnostic instruments, Scotland, UK) was used to capture images. The number of T-Ag positive cells as BKV infected cells and the number of DAPI stained nuclei as total cell numbers were counted automatically by the MetaVue™ Imaging System (Sunnyvale, CA), and the percentage of infected cells was calculated by using formula shown below.

*Percentage of infected cells = number of T – Ag positive cells / number of DAPI stained nuclei × 100.*

To investigate the colocalization of labeled BKV with ER or GA, HRPTEC were incubated with labeled BKV at MOI 5 FFU/cell from 2 to 16 hours at 37 °C. A confocal microscope (Leica TCS SP5) was used to observe cells and Leica application suite advanced fluorescence was used to capture images. Colocalization area and viral particles area were recognized by the MetaVue™ Imaging System and colocalization rate was calculated by using formula shown below.

*Colocalization rate = Area of viral particles colocalized with ER or GA / Area of total viral particles × 100.*

### Statistical analysis

All experiments were repeated at least twice. Means ± SE was calculated from repeated data. A factorial analysis of variance was used to compare western blot analysis and the percentage of infected cells. Linear contrasts were used to test for trend and multiple comparisons used the sidak method for adjustment. The comparison of the colocalization rate over time, used a two-factor repeated measures anova.

### Acknowledgements

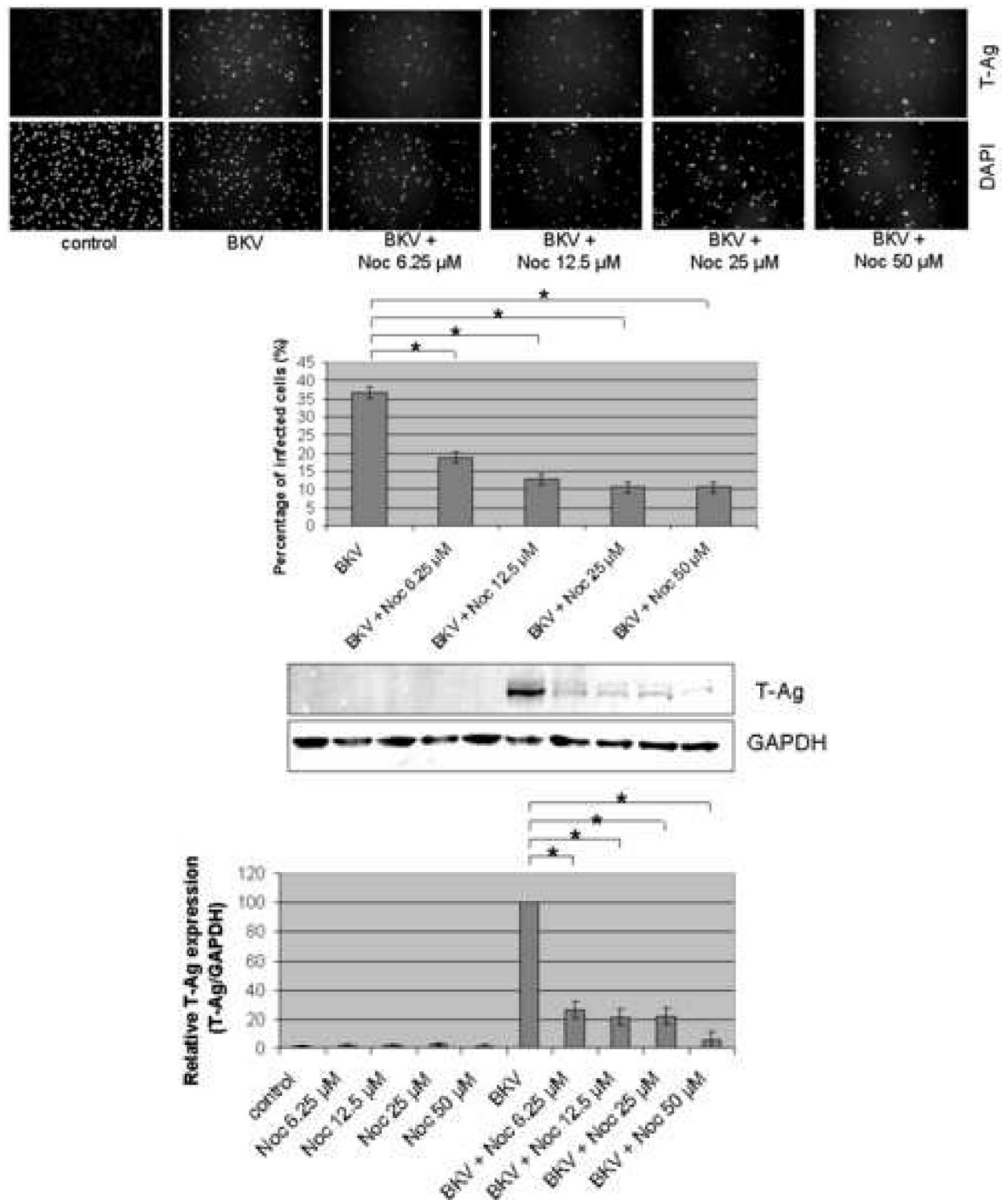
We thank Dr. Raymond Hoffmann (MCW) for help with statistical analysis and Dr. Tetsuro Wakatsuki (MCW) for assistance with co-localization study. We are grateful to Dr. Simon Prosser (MCW) for critical reading and correcting this manuscript. This work was supported by a Program Development Grant from Department of Medicine, Medical College of Wisconsin (A.S.) and NIH R01 HL022563 (A.S.).

### REFERENCES

- Ashok A, Atwood WJ. Constrasting roles of endosomal pH and the cytoskeleton in infection of human glial cells by JC virus and simian virus 40. *J. Virol* 2003;77(2):1347–1356. [PubMed: 12502851]
- Arasaki K, Uemura T, Tani K, Tagaya M. Correlation of Golgilocalization od ZW10 and centrosomal accumulation of dynactin. *Biochem. Biophys. Res. Commn* 2007;359(3):811–816.
- Bernacchi S, Mueller G, Langowski J, Waldeck W. Characterization of simian virus 40 on its infectious entry pathway in cells using fluorescence correlation spectroscopy. *Biochem. Soc. Trans* 2004;32(5):746–749. [PubMed: 15494004]
- Bouchard P, Penningroth SM, Cheung A, Gagnon C, Bardin CW. Erythro-9-[3-(hydroxynonyl)]adenine is an inhibitor of sperm motility that blocks dynein ATPase and protein carboxylmethylase activities. *Proc. Natl. Acad. Sci. USA* 1981;78(2):1033–1036. [PubMed: 6453342]
- Burkhardt JK, Echeverri CJ, Nilsson T, Vallee RB. Overexpression of the dynamitin (p50) subunit of the dynactin complex disrupts dynein-dependent maintenance of membrane organelle distribution. *J. Cell. Biol* 1997;139(2):469–484. [PubMed: 9334349]
- Chen Y, Norkin LC. Extracellular simian virus 40 transmits a signal that promotes virus enclosure within caveolae. *Exp. Cell. Res* 1999;246(1):83–90. [PubMed: 9882517]
- Cheung PY, Zhang Y, Long J, Lin S, Zhang M, Jiang Y, Wu Z. p150<sup>Glued</sup>, dynein, and microtubules are specifically required for activation of MKK3/6 and p38 MAPK. *J. Biol. Chem* 2004;279(44):45308–45311. [PubMed: 15375157]
- Dhani SU, Mohammad-Panah R, Ahmed N, Ackerley C, Ramjeesingh M, Bear CE. Evidence for a functional interaction between the CIC-2 chloride channel and the retrograde motor dynein complex. *J. Biol. Chem* 2003;278(18):16262–16270. [PubMed: 12601004]

- Damm EM, Pelkmans L. Systems biology of virus entry in mammalian cells. *Cell. Microbiol* 2006;8(8): 1219–1227. [PubMed: 16803584]
- Drachenberg CB, Papadimitriou JC, Wali R, Cubitt CL, Ramos E. BK polyoma virus allograft nephropathy: Ultrastructural features from viral cell entry to lysis. *Am. J. Transplant* 2003;3(11): 1383–1392. [PubMed: 14525599]
- Dugan AS, Eash S, Atwood WJ. An N-linked glycoprotein with  $\alpha(2,3)$ -linked sialic acid is a receptor for BK virus. *J. Virol* 2005;79(22):14442–14445. [PubMed: 16254379]
- Dugan AS, Eash S, Atwood WJ. Update on BK virus entry and intracellular trafficking. *Transpl. Infect. Dis* 2006;8(2):62–67. [PubMed: 16734628]
- Eash S, Atwood WJ. Involvement of cytoskeletal components in BK virus infectious entry. *J. Virol* 2005;79(22):11734–11741. [PubMed: 16140751]
- Eash S, Querbes W, Atwood WJ. Infection of vero cells by BK virus is dependent on caveolae. *J. Virol* 2004;78(21):11583–11590. [PubMed: 15479799]
- Gilbert J, Benjamin T. Uptake pathway of polyomavirus via ganglioside GD1a. *J. Virol* 2004;78(22): 12259–12267. [PubMed: 15507613]
- Gilbert JM, Benjamin T. Early steps of polyomavirus entry into cells. *J. Virol* 2000;74(18):8582–8588. [PubMed: 10954560]
- Gilbert JM, Goldberg IG, Benjamin TL. Cell penetration and trafficking of polyomavirus. *J. Virol* 2003;77(4):2615–2622. [PubMed: 12552000]
- Greber UF, Way M. A superhighway to virus infection. *Cell* 2006;124(4):741–754. [PubMed: 16497585]
- Hamm-Alvarez SF, Alayof BE, Himmel HM, Kim PY, Crews AL, Strauss HC, Sheetz MP. Coordinate depression of bradykinin receptor recycling and microtubule-dependent transport by taxol. *Proc. Natl. Acad. Sci. USA* 1994;91(16):7812–7816. [PubMed: 7914372]
- Hamm-Alvarez SF, Kim PY, Sheetz MP. Regulation of vesicle transport in CV-1 cells and extracts. *J. Cell. Sci* 1993;106(3):955–966. [PubMed: 7905879]
- Hamm-Alvarez SF, Sonee M, Loran-Goss K, Shen WC. Paclitaxel and nocodazole differentially alter endocytosis in cultured cells. *Pham. Res* 1996;13(11):1647–1656.
- Leopold PL, Pfister KK. Viral strategies for intracellular trafficking: Motors and microtubules. *Traffic* 2006;7(5):516–523. [PubMed: 16643275]
- Lilley BN, Gilbert JM, Ploegh HL, Benjamin TL. Murine polyomavirus requires the endoplasmic reticulum protein derlin-2 to initiate infection. *J. Virol* 2006;80(17):8739–8744. [PubMed: 16912321]
- Low JA, Magnuson B, Tsai B, Imperiale MJ. Identification of gangliosides GD1b and GT1b as receptors for BK virus. *J. Virol* 2006;80(3):1361–1366. [PubMed: 16415013]
- Low J, Humes HD, Szczyпка M, Imperiale M. BKV and SV40 infection of human kidney tubular epithelial cells in vitro. *Virology* 2004;323(2):182–188. [PubMed: 15193914]
- Mannová P, Forstová J. Mouse polyomavirus utilizes Relcycling endosomes for a trafficking pathway independent COPI vesicle transport. *J. Virol* 2003;77(3):1672–1681. [PubMed: 12525601]
- Marsh M, Helenius A. Virus Entry: Open Sesame. *Cell* 2006;124(4):729–740. [PubMed: 16497584]
- Moriyama T, Wakatsuki T, Sorokin A. Caveolae endocytosis is critical for BKV infection of human renal proximal tubular epithelial cells. *J. Virol* 2007;81(16)in press
- Nichols B. Caveosomes and endocytosis of lipid rafts. *J. Cell. Sci* 2003;116(23):4707–4714. [PubMed: 14600257]
- Norkin LC, Anderson HA, Wolfrom SA, Oppenheim A. Caveolar endocytosis of simian virus 40 is followed by brefeldin A-sensitive transport to the endoplasmic reticulum, where the virus disassembles. *J. Virol* 2002;76(10):5156–5166. [PubMed: 11967331]
- Norkin LC, Kuksin D. The caveolae-mediated SV40 entry pathway bypasses the golgi complex en route to the endoplasmic reticulum. *Virology* 2005;2(38)
- Pelkmans L. Secrets of caveolae- and lipid raft-mediated endocytosis revealed by mammalian cells. *Biochim. Biophys. Acta* 2005;1746(3):295–304. [PubMed: 16126288]
- Pelkmans L, Helenius A. Endocytosis via caveolae. *Traffic* 2002;3(5):311–320. [PubMed: 11967125]
- Pelkmans L, Helenius A. Insider information: what viruses tell us about endocytosis. *Curr. Opin. Cell. Biol* 2003;15(4):414–422. [PubMed: 12892781]

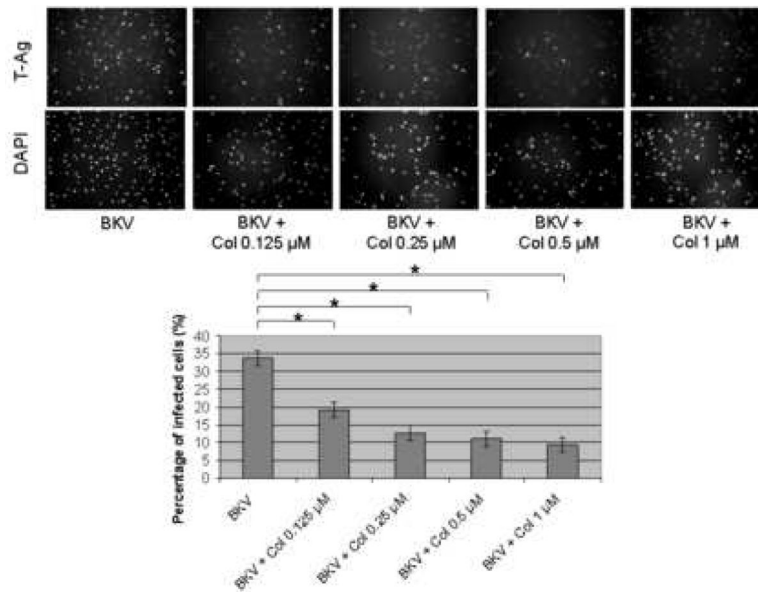
- Pelkmans L, Kartenbeck J, Helenius A. Caveolae endocytosis of simian virus 40 reveals a new two step vesicular transport pathway to the ER. *Nat. Cell. Biol* 2001;3(5):473–483. [PubMed: 11331875]
- Pelkmans L, Pünterner D, Helenius A. Local actin polymerization and dynamin recruitment in SV40-induced internalization of caveolae. *Science* 2002;296(5567):535–539. [PubMed: 11964480]
- Pfeffer SR. Caveolae on the move. *Nat. Cell. Biol* 2001;3(5):E108–110. [PubMed: 11331891]
- Pho MT, Ashok A, Atwood WJ. JC Virus enters human glial cells by clathrin-dependent receptor-mediated endocytosis. *J. Virol* 2000;74(5):2288–2292. [PubMed: 10666259]
- Pietiäinen VM, Marjomäki V, Heino J, Hyypiä T. Viral entry, lipid rafts and caveosomes. *Ann. Med* 2005;37(6):394–403. [PubMed: 16203612]
- Presley JF, Cole NB, Schroer TA, Hirschberg K, Zaal KJM, Lippincott-Schwartz J. ER-to-Golgi transport visualized in living cells. *Nature* 1997;389(4):81–85. [PubMed: 9288971]
- Radtke K, Döhner K, Sodeik B. Viral interactions with the cytoskeleton: a hitchhiker's guide to the cell. *Cell. Microbiol* 2006;8(3):387–400. [PubMed: 16469052]
- Richards AA, Stang E, Pepperkok R, Parton RG. Inhibitors of COP-mediated transport and cholera toxin action inhibit simian virus 40 infection. *Mol. Biol. Cell* 2002;13(5):1750–1764. [PubMed: 12006667]
- Richterová Z, Liebl D, Horák M, Palková Z, Štokrová J, Hozák P, Korb J, Forstová J. Caveolae are involved in the trafficking of mouse polyomavirus virions and artificial VP1 pseudocapsids toward cell nuclei. *J. Virol* 2001;75(22):10880–10891. [PubMed: 11602728]
- Sanjuan N, Porrás A, Otero J. Microtubule-dependent intracellular transport of murine polyomavirus. *Virology* 2003;313(1):105–1006. [PubMed: 12951025]
- Sonee M, Barrón E, Yarber FA, Hamm-Alvarez SF. Taxol inhibits endosomal-lysosomal membrane trafficking at two distinct steps in CV-1 cells. *Am. J. Physiol. Cell. Physiol* 1998;275(6):C1630–1639.
- Tagawa A, Mezzacasa A, Hayer A, Longatti A, Pelkmans L, Helenius A. Assembly and trafficking of caveolar domains in the cell: caveolae as stable, cargo-triggered, vesicular transporters. *J. Cell. Biol* 2005;170(5):769–779. [PubMed: 16129785]
- Zhou J, Gissmann L, Zentgraf H, Müller H, Pickenš M, Müller M. Early phase in the infection of cultured cells with papillomavirus virions. *Virology* 1995;214(1):167–176. [PubMed: 8525612]

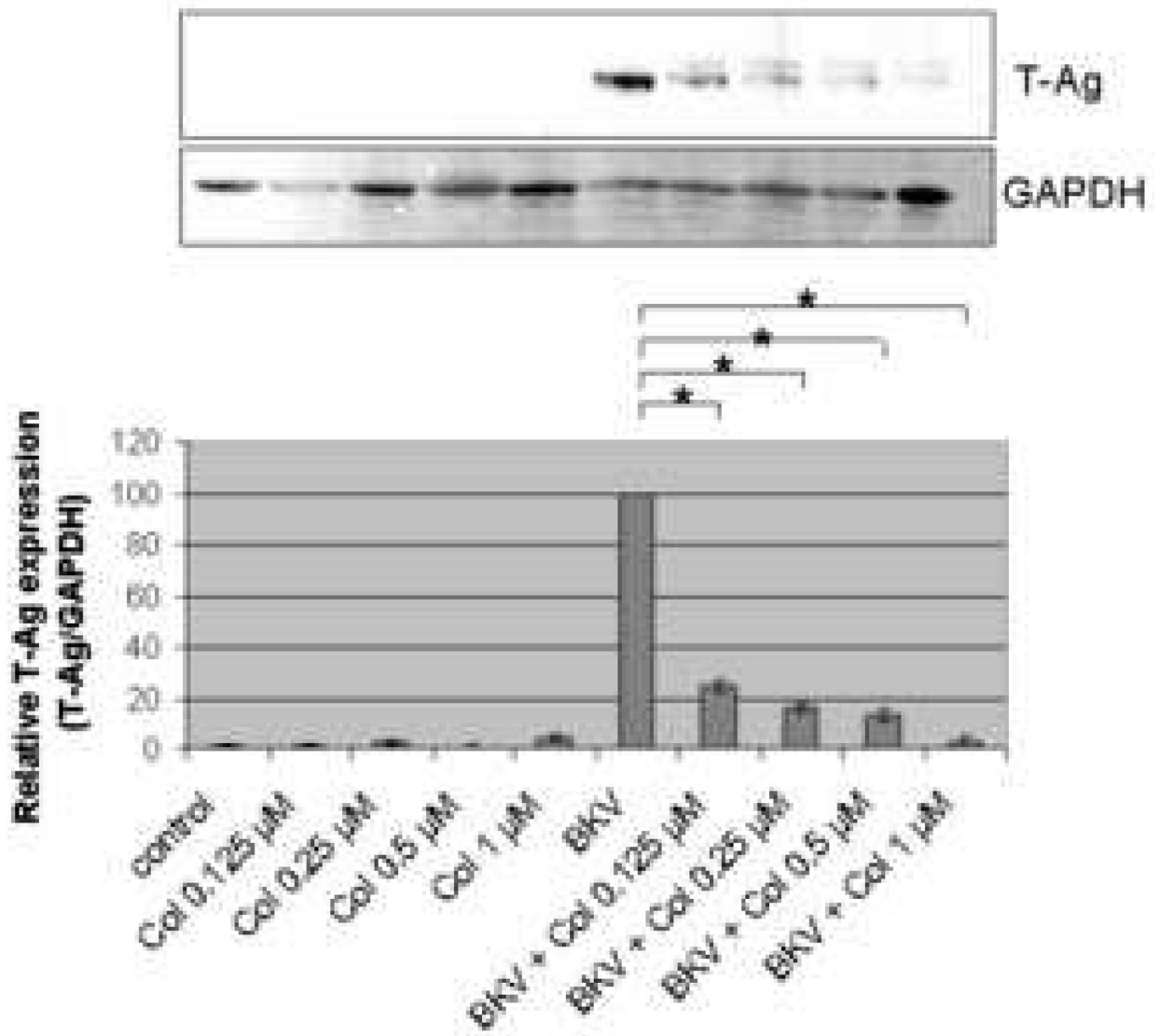


### FIGURE 1. Noc interfered with BKV infection

HRPTEC were pre-incubated with Noc (6.25, 12.5, 25, and 50  $\mu$ M) for 1 hour prior to co-incubation with BKV (MOI 0.5 FFU/cell) and Noc. After 72 hours medium was removed, cells were washed three times with REBM with 0.5 % FBS and incubated for another 48 hours with fresh medium containing Noc. (A) After incubation, cells were fixed and analyzed by IF (Magnification  $\times$ 20). T-Ag positive cells were counted as BKV infected cells and DAPI stained nuclei were counted as total cells. Untreated HRPTEC (control) and HRPTEC incubated with only BKV (BKV) were used as negative and positive controls. At least 500 cells were counted

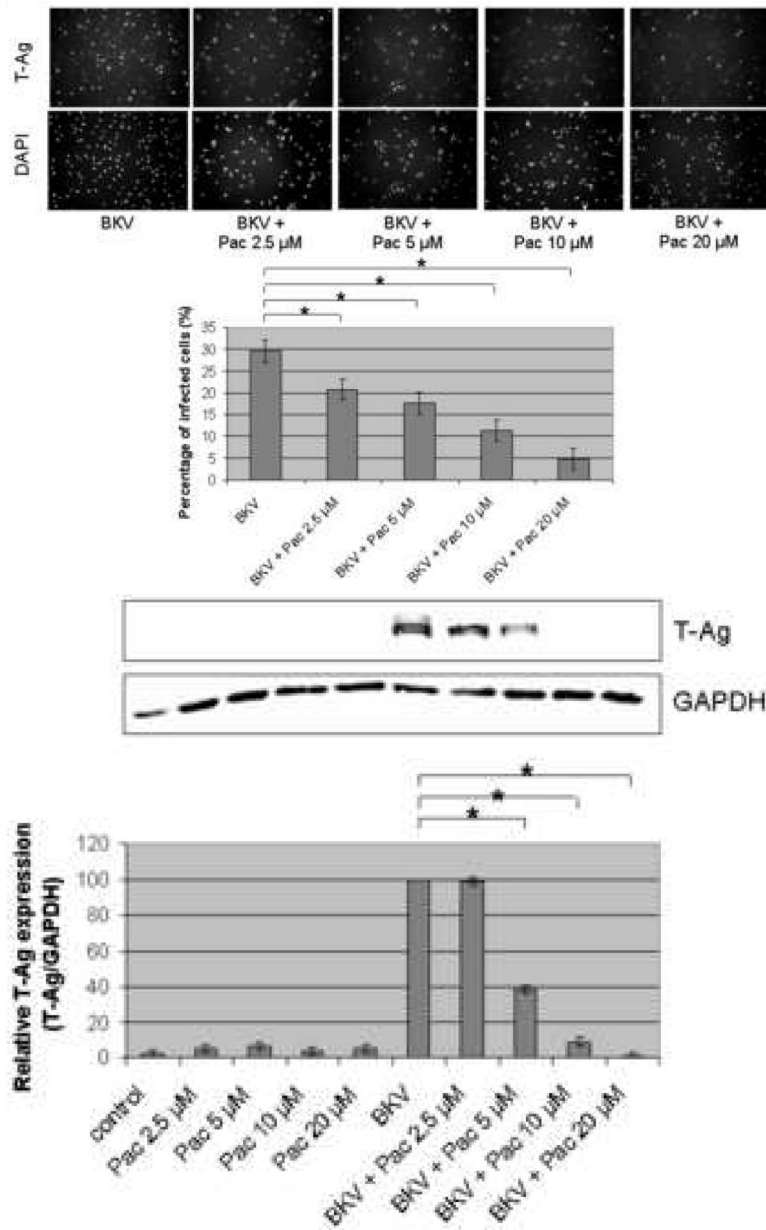
from each three independent cover slips and means and SE were calculated from two independent experiments. \*:  $P < 0.001$ . (B) After incubation, cells were harvested and analyzed by WB. Relative T-Ag expression was expressed as graph bars following measurement of band intensity by Odyssey®. Relative intensity of T-Ag expression was normalized using the intensity of GAPDH as loading control. Means and SE were calculated from two independent experiments. \*:  $P < 0.001$ .





#### FIGURE 2. Col interfered with BKV infection

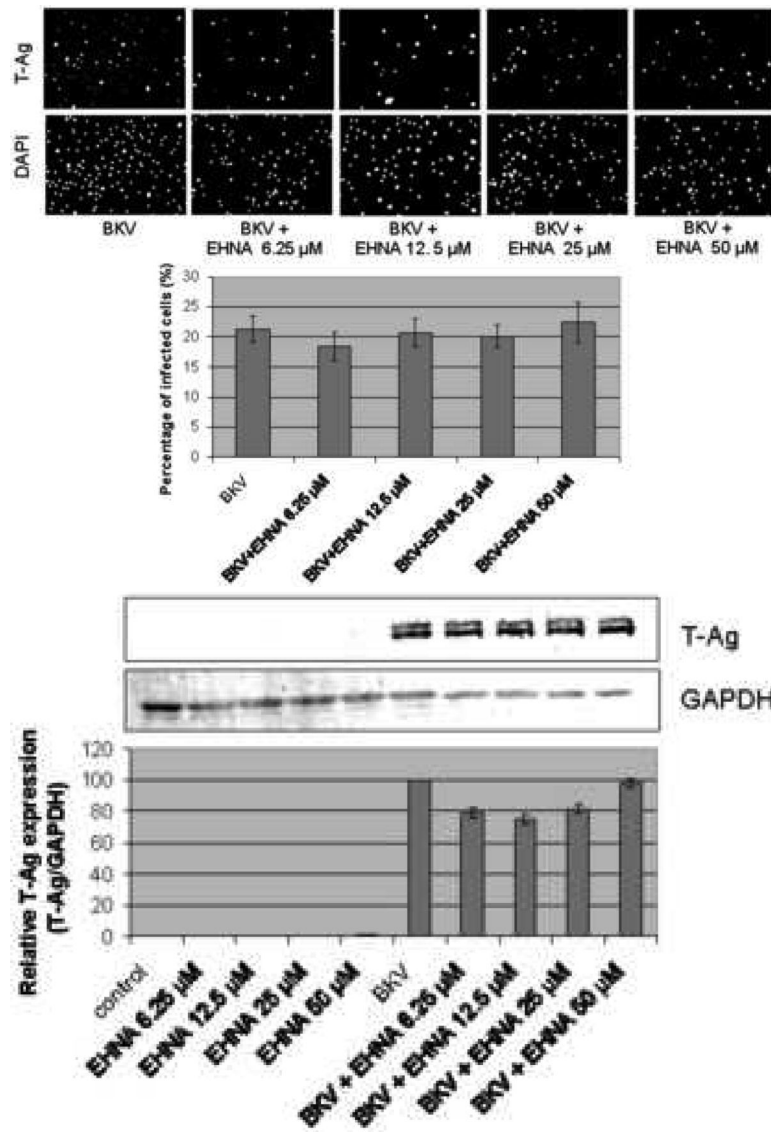
HRPTEC were pre-incubated with Col (0.125, 0.2, 0.5, and 1  $\mu$ M) for 1 hour prior to co-incubation with BKV (MOI 0.5 FFU/cell) and Col for 72 hours. Medium was removed, cells were washed three times with REBM with 0.5 % FBS and incubated for another 48 hours with fresh medium containing Col. (A) After incubation, cells were fixed and analyzed by IF (Magnification  $\times$ 20). T-Ag positive cells were counted as BKV infected cells and the percentage was calculated against DAPI stained nuclei as total cells. At least 500 cells were counted from each three independent cover slips and means and SE were calculated from two independent experiments. \*:  $P < 0.001$ . (B) After incubation, cells were harvested and analyzed by WB. Relative T-Ag expression was detected as graph bars by measurement the intensity by Odyssey<sup>®</sup>. Intensity of T-Ag expression was revised by the intensity of GAPDH as loading control. Means and SE were calculated from two independent experiments. \*:  $P < 0.001$ . Control stands for HRPTEC neither incubated with BKV nor Col. BKV stands for HRPTEC incubated with BKV alone.

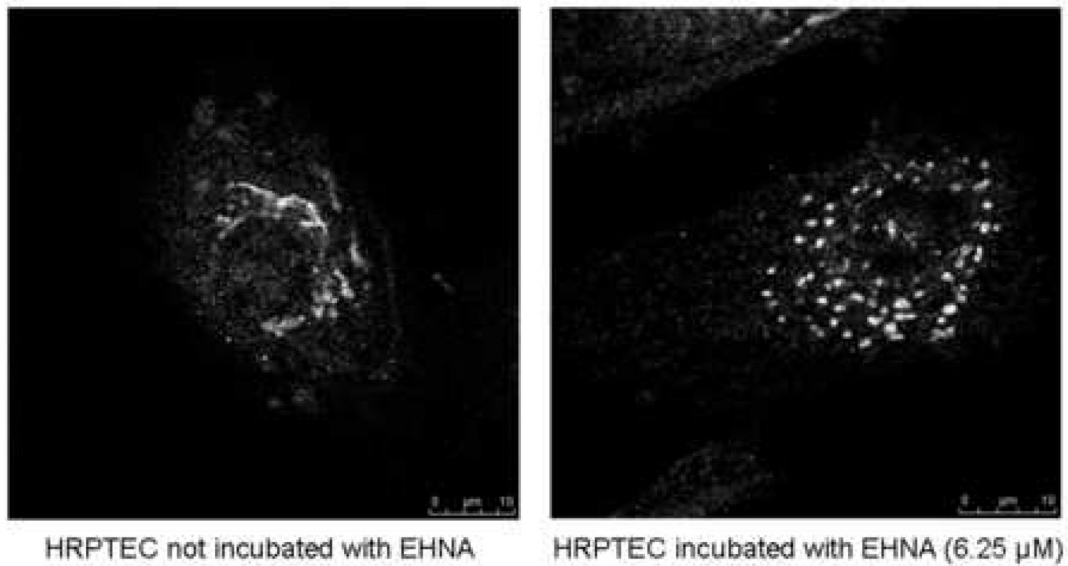


### FIGURE 3. Pac interfered with BKV infection

HRPTEC were pre-incubated of Pac (2.5, 5, 10, and 20 μM) for 1 hour prior to co-incubation with BKV (MOI 0.5 FFU/cell) and Pac for 72 hours. Medium was removed, cells were washed three times with REBM with 0.5 % FBS and incubated for another 48 hours with fresh medium containing Pac. (A) After incubation, cells were fixed and analyzed by IF (Magnification ×20). T-Ag positive cells were counted as BKV infected cells and the percentage was calculated against DAPI stained nuclei as total cells. At least 500 cells were counted from each three independent cover slips and means and SE were calculated from three independent experiments. \*: P<0.001. (B) After incubation, cells were harvested and analyzed by WB. Relative T-Ag expression was detected as graph bars by measurement the intensity by Odyssey®. Intensity of T-Ag expression was revised by the intensity of GAPDH as loading control. Means and SE were calculated from three independent experiments. \*: P<0.001.

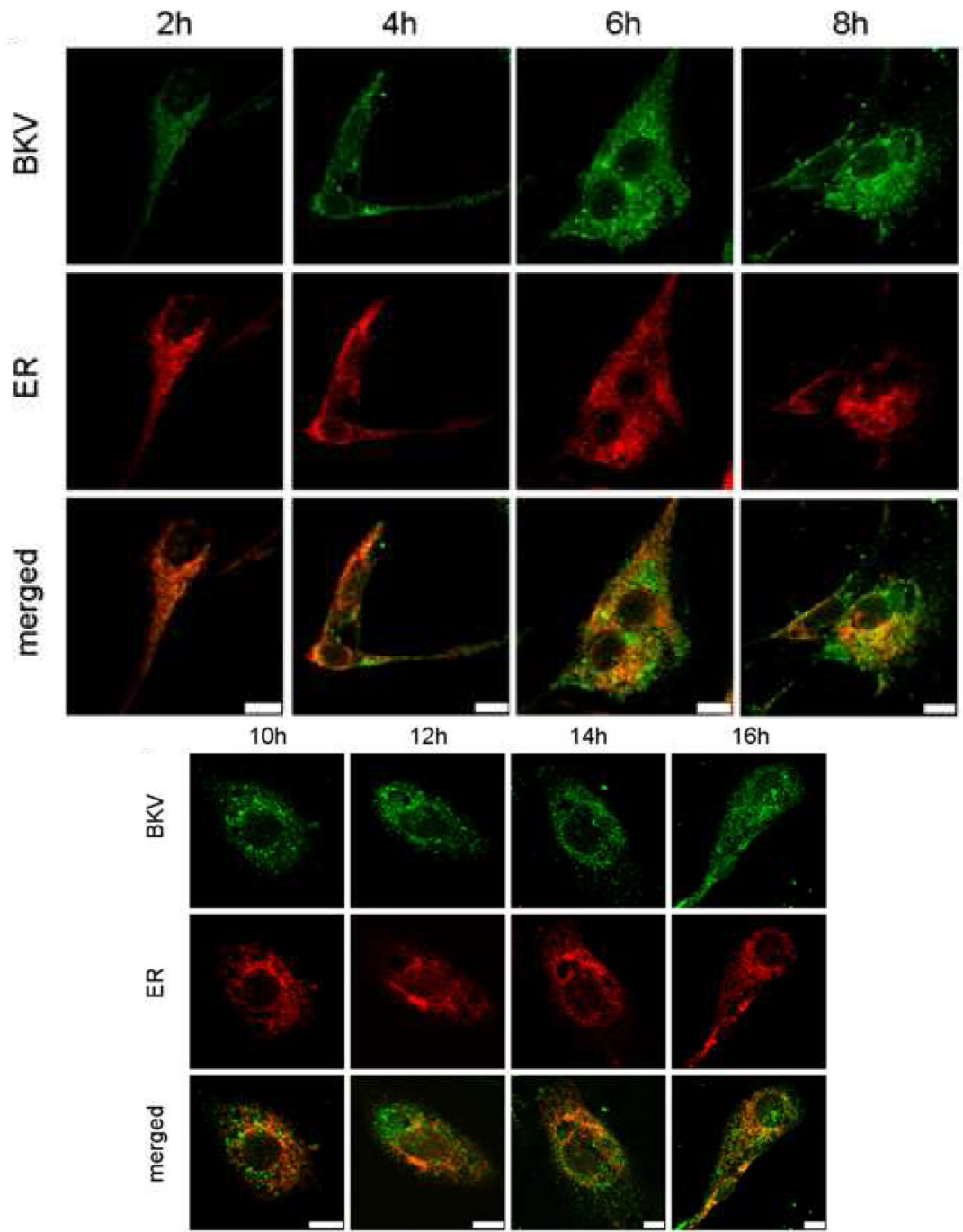
Control stands for HRPTEC neither incubated with BKV nor Pac. BKV stands for HRPTEC incubated with BKV alone.

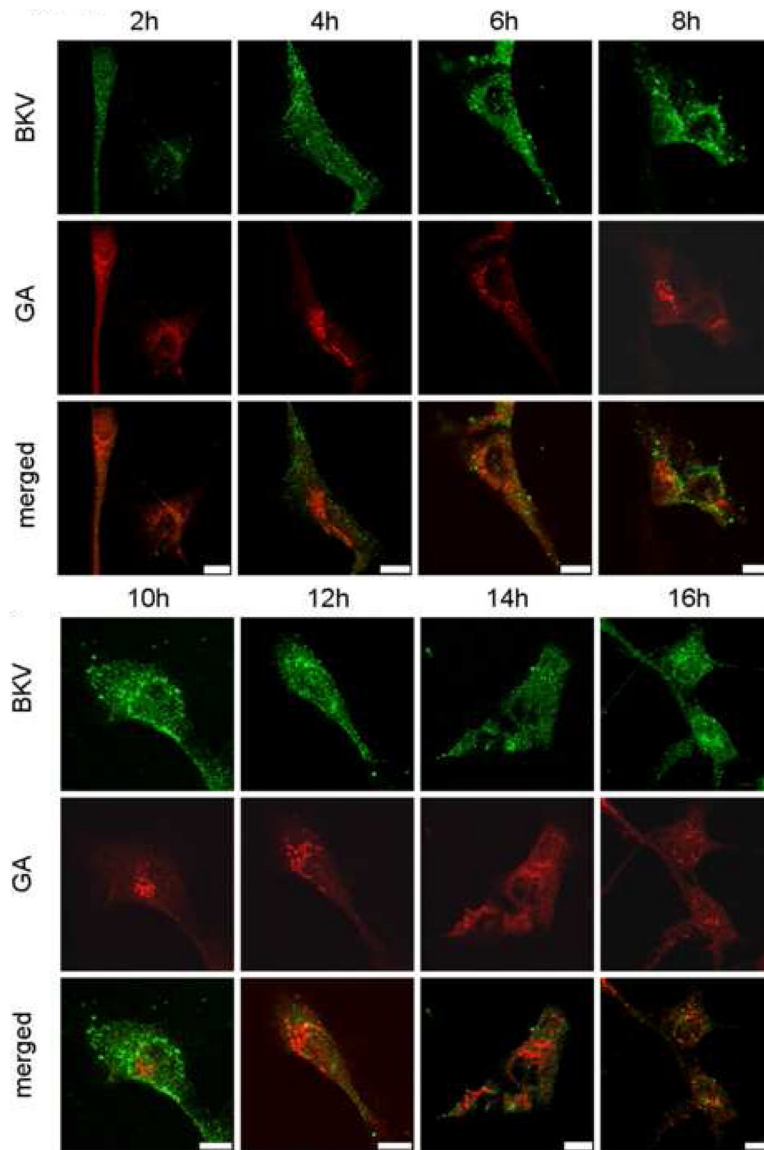




**FIGURE 4. EHNA was not required for BKV infection**

HRPTEC were pre-incubated EHNA (6.25, 12.5, 25, and 50  $\mu$ M) for 1 hour prior to co-incubation with BKV (MOI 0.5 FFU/cell) and EHNA for 72 hours. Medium was removed, cells were washed three times with REBM with 0.5 % FBS and incubated for another 48 hours with fresh medium containing EHNA. (A) After incubation, cells were fixed and analyzed by IF (Magnification  $\times$ 20). T-Ag positive cells were counted as BKV infected cells and the percentage was calculated against DAPI stained nuclei as total cells. At least 500 cells were counted from each three independent cover slips and means and SE were calculated from two independent experiments. (B) After incubation, cells were harvested and analyzed by WB. Relative T-Ag expression was expressed as graph bars following measurement of the band intensity by Odyssey<sup>®</sup>. Relative Intensity of T-Ag expression was normalised by the use of GAPDH band intensity as loading control. Means and SE were calculated from two independent experiments. In this instance control means HRPTEC not incubated with either BKV or EHNA. BKV means HRPTEC incubated with BKV alone. (C) HRPTEC were incubated with or without several doses (6.25, 12.5, 25, and 50  $\mu$ M) of EHNA for 5 days. After incubation, cells were fixed, immunofluoresced by Golgi marker Mannosidase II and analyzed by confocal microscope with 63 $\times$  objective lens. Bars are 10  $\mu$ m.





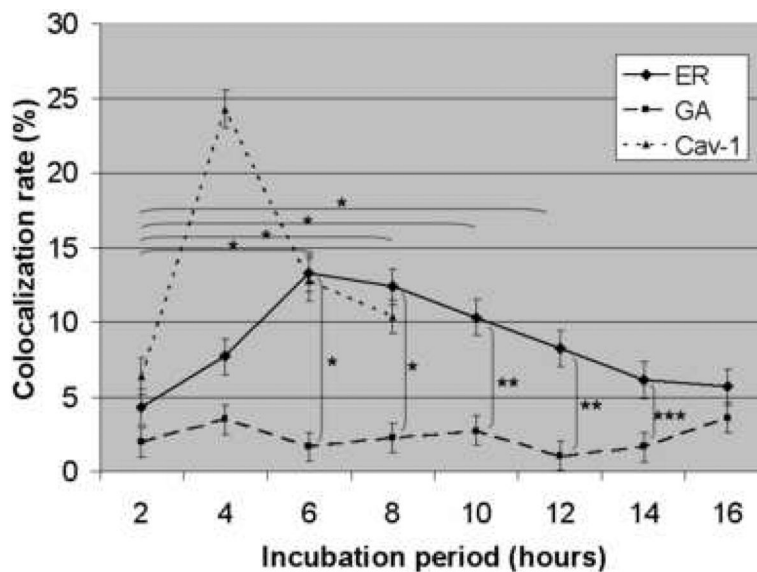


**FIGURE 5. Colocalization of labeled BKV with ER or GA**

(A)(B) Colocalization of BKV with ER or GA. HRPTEC were incubated with Alexa Fluor™ 488 labeled BKV (green) from 2 to 16 hours. After incubation, cells were fixed, immunofluorescenced by ER marker PDI (red) (A) or Golgi marker Mannosidase II (red) (B) and analyzed by confocal microscope with 63× objective lens. Bars are 10 μm. Colocalized labeled BKV particles with ER or GA were expressed as yellow pixels in merged image. (C) Time course and quantitative analysis of colocalization Colocalization rate of labeled BKV with ER or GA were calculated from at least 100 cells random selected from three independent experiments and evaluated from each indication period. Colocalization threshold and viral particle threshold was determined automatically by finding the higher intensity value for yellow pixels and green pixels. Means and SE were calculated from at least two independent experiments. \*: P<0.0001, \*\*: P<0.001, \*\*\*: P<0.01.